

Secondary relaxation in the THz range in 2-adamantanone from theory and experiments

Bingyu Cui¹, Jonathan F. Gebbia², Michela Romamini², Svemir Rudić³, Ricardo Fernandez-Perea⁴, F. Javier Bermejo⁴, Josep-Lluís Tamarit², Alessio Zaccone^{1,5,6}

¹*Cavendish Laboratory, University of Cambridge,
JJ Thomson Avenue, CB3 0HE Cambridge, U.K.*

²*Grup de Caracterizació de Materials, Departament de Física, EEBE and
Barcelona Research Center in Multiscale Science and Engineering,
Universitat Politècnica de Catalunya, Eduard Maristany, 10-14, 08019 Barcelona, Catalonia*

³*ISIS Facility, Rutherford Appleton Laboratory, Chilton,
Didcot, Oxfordshire OX11 0QX, United Kingdom*

⁴*Instituto de Estructura de la Materia, C.S.I.C.,*

Consejo Superior de Investigaciones Científicas, Serrano 123, 28006 Madrid, Spain

⁵*Statistical Physics Group, Department of Chemical Engineering and Biotechnology,
University of Cambridge, Philippa Fawcett Drive, CB3 0AS Cambridge, U.K. and*

⁶*Department of Physics “A. Pontremoli”, University of Milan, via Celoria 16, 20133 Milano, Italy*

We applied the recently developed Generalized Langevin Equation (GLE) approach for dielectric response of liquids and glasses to link the vibrational density (VDOS) of states to the dielectric response of a model orientational glass (OG). The dielectric functions calculated based on the GLE, with VDOS obtained in experiments and simulations as inputs, are compared with experimental data for the paradigmatic case of 2-adamantanone at various temperatures. The memory function is related to the integral of the VDOS times a spectral coupling function $\gamma(\omega_p)$, which tells the degree of dynamical coupling between molecular degrees of freedom at different eigenfrequencies. With respect to previous empirical fittings, the GLE-based fitting reveals a broader temperature range over which the secondary relaxation is active. Furthermore, the theoretical analysis provides a clear evidence of secondary relaxation being localized within the THz (0.5 – 1 THz) range of eigenfrequencies, and thus not too far from the low-energy modes involved in α -relaxation. In the same THz region, the same material displays a crowding of low-energy optical modes that may be related to the secondary relaxation.

INTRODUCTION

The dynamics of structural glasses (SG), those obtained by cooling or pressurizing the liquid state, is one of the major unsolved topics in condensed matter physics [1–4]. In addition to the inescapable collective structural (α) relaxation, a faster (β) secondary relaxation often appears [5–8]. Such a process emerges in the susceptibility function as a separate peak or as an excess (shoulder) contribution to the main α -relaxation. Johari and Goldstein [9, 10] revealed that such a process is an intrinsic dynamical process associated with non-cooperative local reorientations and must be differentiated from relaxations attributed to internal molecular degrees of freedom. In spite of the huge amount of experimental and simulations studies [2, 4–9, 11, 12] as well as the existence of models [13–17] aimed at the understanding of this secondary relaxation, the physics behind is still under discussion. Two main interpretations are generally assumed, the existence of islands of mobility (involving only local regions, so a heterogeneous picture) and the alternative homogeneous interpretation in which molecules show small-angle reorientational diffusion. Whatever the interpretation assumed, the microscopic origin and the relation with low-energy eigenmodes of the system, i.e. optical modes, has not been tried out. This is commonly

due to the difficulty to access different kinds of disorder appearing in SG, i.e., translational and orientational disorder, besides the conformational molecular disorder or internal molecular degrees of freedom. One strategy to simplify the problem is to reduce, as far as possible, the number of degrees of freedom of the studied system.

Under this premise, orientationally disordered (OD) phases (plastic crystal phases) giving rise to orientation glasses (OG) are not affected by the translational disorder [18–21] but still keep the orientational disorder large enough to be controlled. By further decreasing the disorder of the system, molecular systems displaying occupational well-defined disorder appear as those with less degrees of freedom [22–29]. In these systems, molecules can occupy well-defined crystallographic sites for which the fractional occupancies are perfectly determined owing to the ergodic assumption. Moreover, for some cases [22, 30], a closely packed ordered phase exists for the same system and, thus, fundamental properties, such as those concerning thermodynamics or those related to the VDOS, are known and can be successfully compared.

This is the case of 2-adamantanone ($C_{10}H_{14}O$, hereinafter called 2O=A). 2O=A is a “rigid” pseudoglobular molecule of C_{2v} symmetry obtained from adamantane by means of the substitution of two hydrogen atoms by one oxygen atom linked to a secondary carbon atom by a

double bond.

The polymorphic behavior of this compound has been described many times in the literature in the past [22, 30–32]. The OD room temperature phase melts at 529 K and exhibits a face-centered-cubic (FCC) structure (space group $Fm\bar{3}m$.) On cooling the OD phase, it transforms at around 178K to an "ordered" low-temperature monoclinic M phase (space group $P2_1/c$) with statistical disorder in the occupancy of oxygen atoms along three different sites (with fractional occupancies of 25%, 25% and 50%), and returns to the OD phase on heating at ca. 205 K. In addition, submitting the 2O=A to a thermal cycling at normal pressure between 150 and 250 K (i.e. around the low-temperature to OD phase transition) a new denser low-temperature (stable) orthorhombic O phase (space group $Cmc2_1$) appears at the expense of the low-temperature (metastable) M phase and the transition temperature from the low-temperature O phase to the OD phase is found to be shifted from 205 K up to 221 K. Regardless the occupational disorder of the M phase and the full ordered character of the O phase, specific heat capacities were determined to be strikingly close [30]. This experimental evidence is coherent and comes from the close similarity of the experimental VDOS measured for both phases [30]. When comparing both VDOS, the fully ordered O phase shows sharper low frequency excitations than the occupationally disordered M phase at energies between 4 and 12 meV (i.e., 1 to 3 THz, the range comprised between low-energy phonons and the low energy localized frequencies, see Fig. 1). It should be noted that the low-energy range for those excitations was initially associated with some mixing of acoustic and optical modes. The excess excitations for the M phase with respect to the O phase then appear only at that low-energy range.

Despite the Kohlrausch stretched-exponential function and its Fourier transform analog Havriliak-Negami function provide the classical empirical functions to describe the slow α relaxation in any type of supercooled systems (SGs, OGs, etc) a different approach from first principles was recently proposed [33]. This simple approach (see next section) was successfully applied to two orientational glasses, Freon 112 and Freon 113 [34], for which the appearance of the secondary β relaxation for Freon 112 was rationalized on the basis of lower and intermediate-energy excitations in the VDOS.

Here, we bring further insights into this complex problem by analyzing the paradigmatic case of 2O=A, i.e. a system with well-defined occupational disorder (M phase) and for which the fully ordered (O) phase is known. By using the modified theoretical model previously developed [34] we are able to account for the secondary relaxation appearing in the disordered M phase of 2O=A as well as the dynamical coupling of molecular disorder as a function of the eigenfrequencies, in particular, those concerning low-energy localized (optical) modes. Even

more, we will demonstrate that the small differences in the VDOS between disordered M and ordered O phases are so subtle (just some optical modes shifted to lower energy for the disordered phase) that the dielectric susceptibility can be reproduced by using either of the two VDOS, despite the glassy features emerge due to the piling up of those optical modes (see also Ref. [35]) at low-energy in the occupationally disordered M phase.

INELASTIC NEUTRON SCATTERING MEASUREMENTS

Vibrational features of monoclinic and orthorhombic phases of 2-adamantanone were studied by means of Inelastic Neutron Scattering (INS) experiments using the TOSCA spectrometer at the ISIS Pulsed Neutron and Muon Source of the Rutherford Appleton Laboratory (Oxfordshire, UK). In addition, DFT lattice dynamics calculations were performed for the stable fully-ordered orthorhombic phase to understand and interpret the INS data (see supplemental information).

The TOSCA indirect geometry time-of-flight spectrometer [36, 37] is characterized with high spectral resolution ($\Delta E/E \sim 1.25\%$) and broad spectral range ($-24 : 4000 \text{ cm}^{-1}$). The sample was placed in thin walled and flat aluminum can (2 mm of thickness). The monoclinic phase was reached upon cooling from room temperature down below 178K and the stable orthorhombic one was found cycling between 150K and 240K for 6 times monitoring the evolution of the growth of the O phase over the M phase. The cycling was done with a controlled speed of heating/cooling (10K/min). For both phases, the sample chamber was cooled down to 10K by a closed cycle refrigerator (CCR) in order to reduce the effect of the Debye–Waller factor on the spectra, and the INS spectra were recorded. Finally, the data were converted to the dynamic structure factor, $S(Q, \omega)$, using the Mantid software framework.

THEORETICAL GLE MODEL

Focusing on a tagged particle (e.g. a molecular subunit carrying a partial charge which reorients under the electric field), it is possible to describe its motion under the applied field using a particle-bath Hamiltonian of the Caldeira-Leggett type, in the classical dynamics regime. The particle's Hamiltonian is bi-linearly coupled to a bath of harmonic oscillators which represent all other molecular degrees of freedom in the system [38]. Any complex system of oscillators can be reduced to a set of independent oscillators by performing a suitable normal mode decomposition. This allows us to identify the spectrum of eigenfrequencies of the system, i.e. the

experimental VDOS, with the spectrum of the set of harmonic oscillators forming the bath.

The particle-bath Hamiltonian under a uniform AC electric field, is given by [33]: $H = H_P + H_B$ where $H_P = P^2/2m + V(Q) - q_e Q E_0 \sin(\omega t)$ is the Hamiltonian of the tagged particle with the external electric field (q_e is the charge carried by the particle), $H_B = \frac{1}{2} \sum_{\alpha=1}^N \left[\frac{P_{\alpha}^2}{m_{\alpha}} + m_{\alpha} \omega_{\alpha}^2 \left(X_{\alpha} - \frac{F_{\alpha}(Q)}{\omega_{\alpha}^2} \right)^2 \right]$ is the Hamiltonian of the bath of harmonic oscillators that are coupled to the tagged particle [38]. H_B consists of two parts: The first part is the ordinary harmonic oscillator; the second is the coupling term between the tagged particle position Q and the bath oscillator position X_{α} . The coupling function is taken to be linear in the displacement of the particle, $F_{\alpha}(Q) = c_{\alpha} Q$, where c_{α} is known as the strength of coupling between the tagged atom and the α -th bath oscillator. Hence, there is a spectrum of coupling constants c_{α} by which each particle interacts with all other molecular degrees of freedom in the system. This spectrum of coupling strengths will play a major role in the subsequent analysis.

As shown in previous work [33, 39], this particle-bath Hamiltonian leads to a Generalized Langevin Equation (GLE) for the mass-rescaled coordinate q of the tagged particle:

$$\ddot{q} = -V'(q) - \int_{-\infty}^t \nu(t') \frac{dq}{dt'} dt' + q_e E_0 \sin(\omega t). \quad (1)$$

where the non-Markovian friction or memory kernel $\nu(t)$ is expressed in terms of the spectrum of coupling constants c_{α} as $\nu(t) = \sum_{\alpha} \frac{c_{\alpha}^2}{\omega_{\alpha}^2} \cos(\omega_{\alpha} t)$.

Then we can let the spectrum be continuous and c_{α} be a function of ω_p which leads to the following expression for the friction kernel [38]:

$$\nu(t) = \int_0^{\infty} d\omega_p D(\omega_p) \frac{\gamma(\omega_p)^2}{\omega_p^2} \cos \omega_p t, \quad (2)$$

where $\gamma(\omega_p)$ is the continuous spectrum of coupling constants, i.e. the continuous version of the discrete set $\{c_{\alpha}\}$.

The inverse cosine transform in turn gives the spectrum of coupling constants $\gamma(\omega_p)$ as a function of the memory kernel:

$$\gamma^2(\omega_p) = \frac{2\omega_p^2}{\pi D(\omega_p)} \int_0^{\infty} \nu(t) \cos(\omega_p t) dt. \quad (3)$$

This coupling function contains information on how strongly the single particle motion is coupled to the motion of other particles in a mode with vibrational frequency ω_p . This is an important information, because it reveals the degree of medium and long-range (anharmonic) couplings in the motion of the molecules.

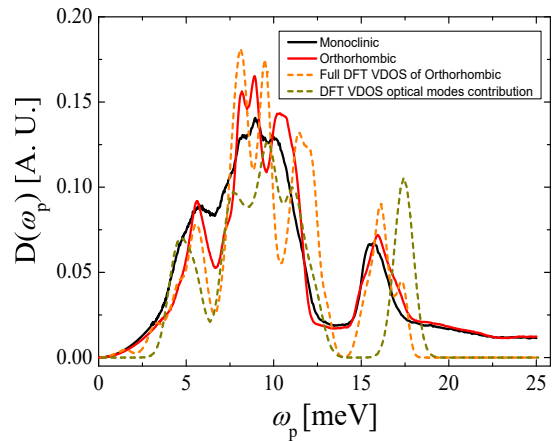


FIG. 1: Vibrational density of states from various approaches for 2-damantanone. Solid lines show experimental INS spectra, black for M phase and red for O phase. Dashed lines show VDOS from DFT lattice dynamic calculations of O phase, orange for VDOS using full phonon dispersion contribution and dark yellow for VDOS with only optical modes contribution.

Following the same steps as those described in Ref. [33], we obtain the complex dielectric function

$$\epsilon^*(\omega) = 1 - A \int_0^{\omega_D} \frac{D(\omega_p)}{\omega^2 - i\omega\tilde{\nu}(\omega) - \omega_p^2} d\omega_p \quad (4)$$

where A is an arbitrary positive rescaling constant, and ω_D is the Debye cut-off frequency (i.e. the highest eigenfrequency in the VDOS spectrum). As one can easily verify, if $D(\omega_p)$ were given by a Dirac delta, one would recover the standard simple-exponential (Debye) relaxation.

The VDOS is an important key input to the theoretical framework. The experimental VDOS, $D(\omega_p)$, of M and O phases, measured at $T = 10K$ by means of inelastic neutron scattering using TOSCA spectrometer are shown in Fig. 1, together with VDOS obtained by DFT *ab-initio* lattice-dynamics calculation for orthorhombic phase at Γ -point (only optical modes contributes to VDOS) as well as using full phonon dispersions (see Supplemental Material). This set of VDOS will be used as the input to explore the effect on the dielectric responses.

RESULTS AND DISCUSSION

Fitting of dielectric loss

When exhibiting secondary β -relaxation in loss modulus of dielectric permittivity, we take the form of memory function $\nu(t)$ in Eq. (1) to be the sum of two terms, both of which are stretched exponential. As in previous work

Temperature	128K	130K	132K	134K	136K	154K	178K	202K
b_1	0.39	0.40	0.40	0.38	0.4	0.46	0.5	0.53
τ_1 (seconds)	418.04	200.47	144.76	69.09	32	0.222	0.0016	$3.50 \cdot 10^{-5}$
b_2	0.225	0.21	0.19	0.18	0.18			
τ_2 (seconds)	$7.4 \cdot 10^{-5}$	$5.00 \cdot 10^{-5}$	$1.77 \cdot 10^{-5}$	$9.60 \cdot 10^{-6}$	$9.60 \cdot 10^{-6}$			
ν_2	0.023	0.021	0.02	0.02	0.025	0	0	0

TABLE I: Parameters of the memory function.

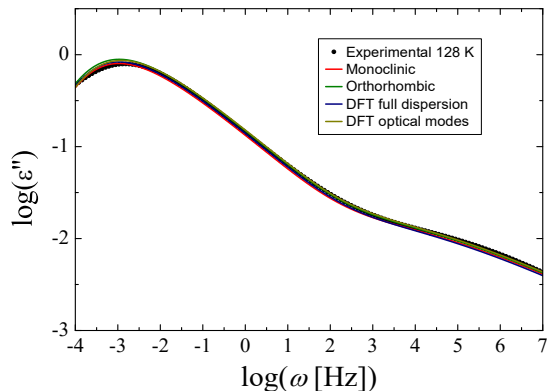


FIG. 2: Fitting of experimental data using the proposed theoretical model for 2-adamantanone at the same temperature with different VDOS as inputs.

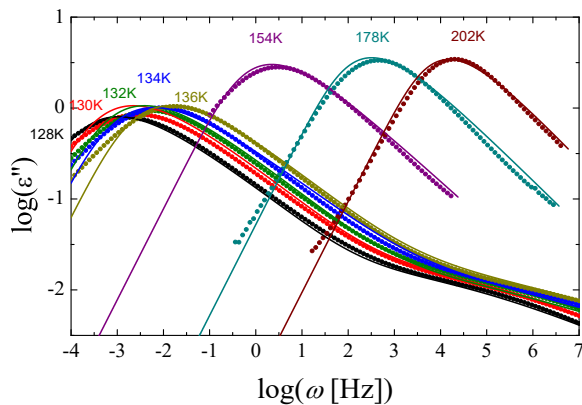


FIG. 3: Fitting of experimental data using the proposed theoretical model for 2-adamantanone at various temperatures with the same (experimental monoclinic) input VDOS.

for the case of Freon 112 [34], we take the following phenomenological expression for our memory function

$$\nu(t) = \nu_0 \sum_i \nu_i e^{-(t/\tau_i)^{b_i}}, \quad (5)$$

where τ_i is a characteristic time-scale, with $i = 1$ for α relaxation and $i = 2$ for β relaxation. ν_0 is a constant prefactor while ν_i with $i = 1, 2$ indicates the weight for the two different stretched exponentials. Without loss of

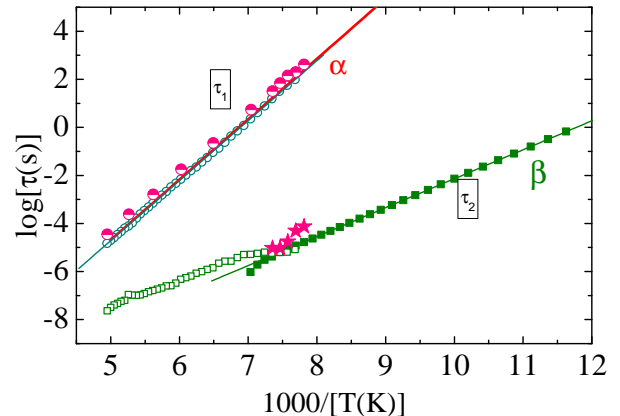


FIG. 4: Relaxation times as a function of reciprocal of temperature for the different relaxation processes: Open circles: α -relaxation (experimental values); open squares: β -relaxation (calculated values according to the CM model (refs [15, 16])); full green squares: beta-relaxation (experimental values). Pink symbols are calculated according to our proposed theoretical model (see Table I): Full-empty circles for α -relaxation and stars for beta relaxation.

generality, we set ν_1 to be unity. Fitting parameters at different temperatures are listed in Table I. To explore the effect of VDOS on dielectric relaxation behaviour, in Fig. 2, we only fit at one temperature at $T = 128K$ with different VDOS in Fig. 1, using the same memory kernel. The results are the same for other temperatures. The differences between the VDOS of the ordered and disordered phases are negligible, such that the procedure can hardly feel differences when comparing the dielectric loss. The calculation using the VDOS calculated from DFT for the ordered phase also provides the same results.

Moreover, an important consideration is that concerning optical modes. Fittings of the experimental data under various temperatures of the dielectric loss modulus with the VDOS of the monoclinic phase are shown in Fig. 3. For the fitting procedure, we have assumed that $D(\omega_p)$ and the overall scaling in the stretched exponential, ν_0 , are temperature-independent. We used the algorithm in [40] to perform the Fourier transform of stretched exponential functions. The so obtained relaxation times are plotted in Fig. 4.

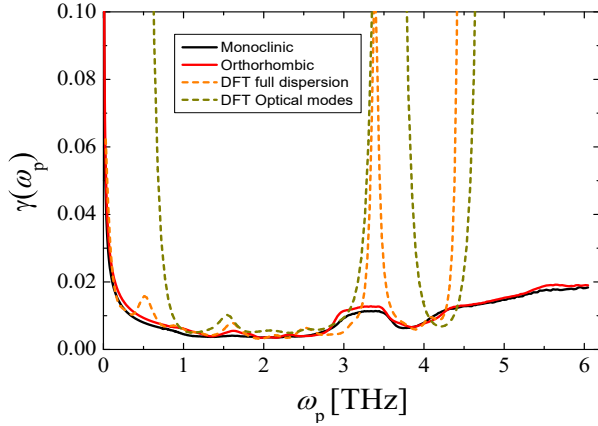


FIG. 5: Spectrum of coupling constants as a function of the vibrational eigenfrequency computed according to Eq. (3) using the same phenomenological memory functions $\nu(t)$ used in the fitting of dielectric response in Fig. 2, with the same color code used for the input VDOS of Fig 1 but the same form of memory kernel.

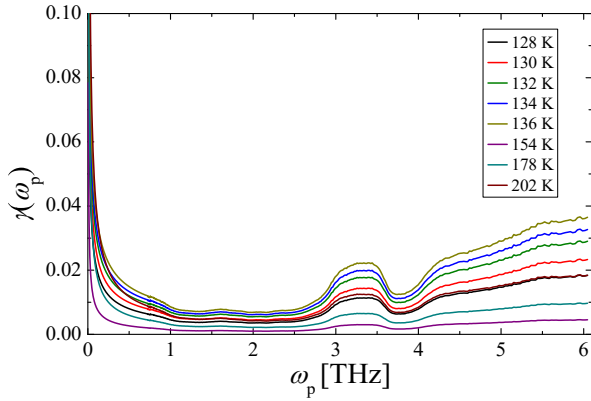
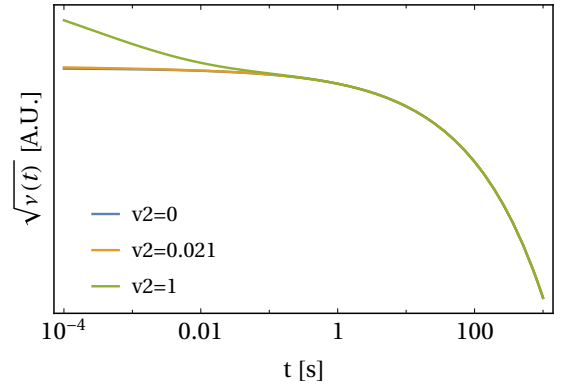


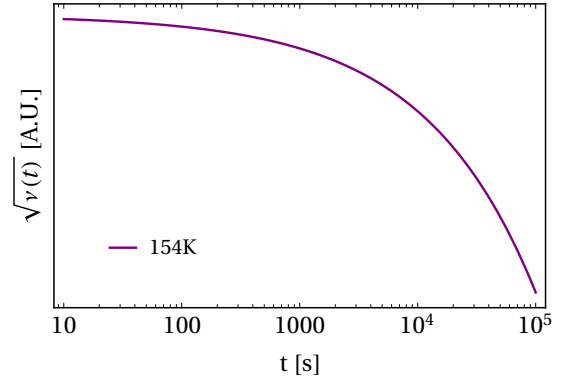
FIG. 6: Spectrum of coupling constants as a function of the vibrational eigenfrequency computed according to Eq. (3) using the phenomenological memory functions $\nu(t)$ used in the fitting of dielectric response in Fig. 3, with same colour setting for the different temperatures.

Analysis of spectrum of dynamic coupling constants

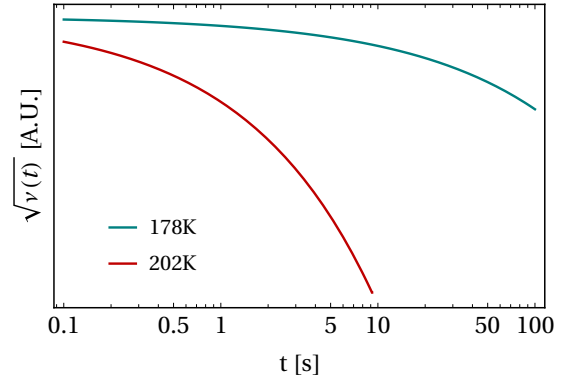
To physically understand secondary relaxation in these systems, the spectrum of dynamical coupling parameters (Eq. (3)) has been analysed (see Fig. 5 and 6). In general, the coupling spectrum decays from the highest Debye cut-off frequency of short-range high-frequency in-cage motions (above 5THz), down to the low eigenfrequency part where the coupling goes up with decreasing ω_p towards zero, due to phonons or phonon-like excitations, which are collective and long-wavelength and hence result in a larger value of coupling parameter γ . The latter region of eigenfrequency is also the one corresponding



(a) Comparing the results of different weight ν_2 .



(b) T=154K



(c) Higher temperature.

FIG. 7: Time decay of the square-root of total memory function for the friction $\nu(t)$ according to the relation $F(q, t) \sim \sqrt{\nu(t)}$. Color settings are the same as in Fig. 3

to α -relaxation. In the intermediate range of vibration frequency (3 – 4THz), fluctuations in the coupling spectrum are observed.

Looking at Fig. 5, at ca. 0.5THz, there is a clear peak for DFT full VDOS, which seems to become a "divergence" for the DFT optical modes due to the optical gap. Effectively, a maximum in VDOS corresponds to a minimum in the coupling and vice versa (whenever there is

a gap in the VDOS there is a divergence in the coupling spectrum³), which is clear in Eq. (3). Because of the sampling of the VDOS (with dispersions), at low-energy there are some numerical fluctuations which cause a pronounced artificial peak at low frequency in coupling. In the case of the VDOS obtained without taking into account the dispersions of the branches (only optical modes contribute to VDOS), there is a gap from 0 to the first optical mode and this causes the divergence in the coupling spectrum. On the other hand, in the experimental orthorhombic and monoclinic data, the coupling appears more attenuated and no divergences are observed.

Analysis of secondary relaxation processes

As shown in previous work [34], secondary relaxation shows up in the plot of dynamic coupling constant in an intermediate range comprised between low-energy phonons and the high-energy localized frequencies at the Debye cut-off.

Searching for the signature of the secondary relaxation process in Fig. 6, we first note that the bump in the intermediate energy range 3-4THz cannot represent a genuine relaxation process because this bump is just the smeared-out version of a highly divergent feature visible in Fig. 5 and due to the presence of an optical gap in the VDOS in that energy range.

Hence, by exclusion, we can identify the emergence of the secondary relaxation as the other bump (or shoulder) in the plot just below 1THz in Fig. 6. The bump is not too far from the steeply increasing tail formed by collective modes active in the phonon-like regime and boson-peak soft modes responsible for α -relaxation [33]. This is also the reason why the contributions of α and secondary relaxation to the ϵ'' curves are not always easily distinguishable, except for the lowest temperatures considered. In particular, it is interesting to observe the opposite behaviour of overall spectrum of coupling constant curves for temperatures above and below $T = 136\text{K}$ (which is comparable with glass transition temperature at $T_g \approx 132\text{K}$). The coupling spectra for temperatures below $T = 136\text{K}$ lie on top of the coupling spectra above $T = 136\text{K}$, which goes along with the fact that the data of dielectric loss in Fig. 3 are deprived of secondary relaxation processes above $T = 136\text{K}$. Hence, the lack of secondary relaxation processes manifests as overall lower in magnitude values of dynamical coupling among degrees of freedom.

Deducing the intermediate scattering function decays from dielectric loss fittings

As shown by Sjoegren and Sjoelander [41] and as discussed in previous work [42], the time-dependence of the

memory function is proportional to the square of the time-dependence of the intermediate scattering function (ISF). Hence, for a process with pure α relaxation there is a simple stretched-exponential decay of the ISF, whereas two decays are produced for systems with both α and β . To model both α and β relaxations under certain temperatures, we take $\nu(t)$ to be the sum of two stretched exponential functions as in Eq. (5) above, with independent parameters, which results in a two-step decay in the ISF.

This behaviour is shown in Fig. 7 following the relation $F(q, t) \sim \sqrt{\nu(t)}$. Since the weight ν_2 used in the fitting for β -relaxation is small, we hardly see the characteristic two-step stretched exponential decay of $F(q, t)$ present in systems with well separated α and β relaxations at low temperatures ($T \leq 136\text{K}$). However, on the other hand, at high temperatures, the α peak in ϵ'' , and the corresponding decay in $F(q, t)$, can be reduced to a single characteristic time, as the time scale range of the α -relaxation contains a strong contribution from soft modes in the VDOS. This is clear from Eq. (3) where the term ω_p^2 in the denominator gives a large weight to the low- ω_p part of the VDOS, which contains the BP-proliferation of soft modes.

CONCLUSION

In conclusion, we have examined, for the paradigmatic case of 2-adamantanone, how its VDOS influences dielectric relaxation. We have found that: (i) only small differences in the VDOS between ordered and disordered phases exist, and can be seen only at very low energy; (ii) such differences concern mostly the optical modes, which for the monoclinic disordered phase are at lower energies; (iii) the piling up of the optical modes at low energy (at least in these organic compounds) are the root cause for the "glassy behavior", but in a very subtle way. Regarding the last point, the role of the optical modes is so subtle that a property directly linked to the VDOS such as the dielectric loss of the disordered phase (experimentally measured) and the "hypothetical" dielectric loss of the orthorhombic fully-ordered phase (not available experimentally) would be the same. Finally, the fitting using the GLE theoretical modes allows one to isolate the energy range of vibrational eigenmodes which participate in the secondary (β) relaxation. This is particularly important in systems like 2-adamantanone where there is no separation between α and secondary relaxations in the dielectric loss. It is seen that the vibrational eigenmodes responsible for secondary relaxation fall in an energy range around 0.5 – 1 THz, which corresponds to the range where soft optical modes appear in the VDOS. This points at an unprecedented link between low-energy optical modes in organic molecular systems and secondary β relaxation, which deserves further investigation in future

work.

B. C acknowledges the financial support of CSC-Cambridge Scholarship. J.Ll. T. acknowledges MINECO (FIS2017-82625-P) and the Catalan government (SGR2017-042) for financial support.

-
- [1] K. Ngai, “Dynamic and thermodynamic properties of glass-forming substances,” *Journal of Non-Crystalline Solids*, vol. 275, no. 1, pp. 7–51, 2000.
- [2] P. G. Debenedetti and F. H. Stillinger, “Supercooled liquids and the glass transition,” *Nature*, vol. 410, no. 6825, p. 259, 2001.
- [3] J. C. Mauro, Y. Yue, A. J. Ellison, P. K. Gupta, and D. C. Allan, “Viscosity of glass-forming liquids,” *Proceedings of the National Academy of Sciences*, vol. 106, no. 47, pp. 19780–19784, 2009.
- [4] C. M. Roland, S. Hensel-Bielowka, M. Paluch, and R. Casalini, “Supercooled dynamics of glass-forming liquids and polymers under hydrostatic pressure,” *Reports on Progress in Physics*, vol. 68, pp. 1405–1478, may 2005.
- [5] J. D. Stevenson and P. G. Wolynes, “A universal origin for secondary relaxations in supercooled liquids and structural glasses,” *Nature Physics*, vol. 6, pp. 62–68, 2010.
- [6] W. Tu, S. Valenti, K. L. Ngai, S. Capaccioli, Y. D. Liu, and L.-M. Wang, “Direct evidence of relaxation anisotropy resolved by high pressure in a rigid and planar glass former,” *The Journal of Physical Chemistry Letters*, vol. 8, no. 18, pp. 4341–4346, 2017. PMID: 28841327.
- [7] A. Vispa, M. Romanini, M. A. Ramos, L. C. Pardo, F. J. Bermejo, M. Hassaine, A. I. Krivchikov, J. W. Taylor, and J. Ll. Tamarit, “Thermodynamic and kinetic fragility of freon 113: The most fragile plastic crystal,” *Phys. Rev. Lett.*, vol. 118, p. 105701, Mar 2017.
- [8] M. Romanini, M. Barrio, R. Macovez, M. D. Ruiz-Martin, S. Capaccioli, and J. Ll. Tamarit, “Thermodynamic scaling of the dynamics of a strongly hydrogen-bonded glass-former,” *Scientific Reports*, vol. 7, p. 1346, 2017.
- [9] G. P. Johari and M. Goldstein, “Viscous liquids and the glass transition. iii. secondary relaxations in aliphatic alcohols and other nonrigid molecules,” *The Journal of Chemical Physics*, vol. 55, no. 9, pp. 4245–4252, 1971.
- [10] G. P. Johari and M. Goldstein, “Viscous liquids and the glass transition. ii. secondary relaxations in glasses of rigid molecules,” *The Journal of Chemical Physics*, vol. 53, no. 6, pp. 2372–2388, 1970.
- [11] K. L. Ngai, P. Lunkenheimer, C. Len, U. Schneider, R. Brand, and A. Loidl, “Nature and properties of the johari-goldstein β -relaxation in the equilibrium liquid state of a class of glass-formers,” *The Journal of Chemical Physics*, vol. 115, no. 3, pp. 1405–1413, 2001.
- [12] N. B. Caballero, M. Zuriaga, J. Ll. Tamarit, and P. Serra, “Dynamic heterogeneity in an orientational glass,” *The Journal of Chemical Physics*, vol. 147, no. 18, p. 184501, 2017.
- [13] M. Domschke, M. Marsilius, T. Blochowicz, and T. Voigtmann, “Glassy relaxation and excess wing in mode-coupling theory: The dynamic susceptibility of propylene carbonate above and below T_c ,” *Phys. Rev. E*, vol. 84, p. 031506, Sep 2011.
- [14] K. Y. Tsang and K. L. Ngai, “Dynamics of relaxing systems subjected to nonlinear interactions,” *Phys. Rev. E*, vol. 56, pp. R17–R20, Jul 1997.
- [15] K. Ngai, “Universality of low-frequency fluctuation, dissipation, and relaxation properties of condensed matter. i,” *Comments Solid State Phys*, vol. 9, no. 4, pp. 127–140, 1979.
- [16] K. L. Ngai, “An extended coupling model description of the evolution of dynamics with time in supercooled liquids and ionic conductors,” *Journal of Physics: Condensed Matter*, vol. 15, pp. S1107–S1125, mar 2003.
- [17] W. Gotze and L. Sjogren, “Relaxation processes in supercooled liquids,” *Reports on Progress in Physics*, vol. 55, pp. 241–376, mar 1992.
- [18] M. A. Ramos, S. Vieira, F. J. Bermejo, J. Dawidowski, H. E. Fischer, H. Schober, M. A. González, C. K. Loong, and D. L. Price, “Quantitative assessment of the effects of orientational and positional disorder on glassy dynamics,” *Phys. Rev. Lett.*, vol. 78, pp. 82–85, Jan 1997.
- [19] R. Brand, P. Lunkenheimer, and A. Loidl, “Relaxation dynamics in plastic crystals,” *The Journal of Chemical Physics*, vol. 116, no. 23, pp. 10386–10401, 2002.
- [20] U. Schneider, R. Brand, P. Lunkenheimer, and A. Loidl, “Excess wing in the dielectric loss of glass formers: A johari-goldstein β relaxation?,” *Phys. Rev. Lett.*, vol. 84, pp. 5560–5563, Jun 2000.
- [21] R. Puertas, M. A. Rute, J. Salud, D. O. López, S. Diez, J. K. van Miltenburg, L. C. Pardo, J. Ll. Tamarit, M. Barrio, M. A. Pérez-Jubindo, and M. R. de la Fuente, “Thermodynamic, crystallographic, and dielectric study of the nature of glass transitions in cyclo-octanol,” *Phys. Rev. B*, vol. 69, p. 224202, Jun 2004.
- [22] M. Romanini, P. Negrier, J. Ll. Tamarit, S. Capaccioli, M. Barrio, L. C. Pardo, and D. Mondieig, “Emergence of glassy-like dynamics in an orientationally ordered phase,” *Phys. Rev. B*, vol. 85, p. 134201, Apr 2012.
- [23] M. Zuriaga, L. C. Pardo, P. Lunkenheimer, J. Ll. Tamarit, N. Veglio, M. Barrio, F. J. Bermejo, and A. Loidl, “New microscopic mechanism for secondary relaxation in glasses,” *Physical Review Letters*, vol. 103, no. 7, p. 075701, 2009.
- [24] S. C. Pérez, M. Zuriaga, P. Serra, A. Wolfenson, P. Negrier, and J. Ll. Tamarit, “Dynamic characterization of crystalline and glass phases of deuterated 1,1,2,2-tetrachloroethane,” *The Journal of Chemical Physics*, vol. 143, no. 13, p. 134502, 2015.
- [25] M. Romanini, M. Barrio, S. Capaccioli, R. Macovez, M. D. Ruiz-Martin, and J. Ll. Tamarit, “Double primary relaxation in a highly anisotropic orientational glass-former with low-dimensional disorder,” *J. Phys. Chem. C*, vol. 120, pp. 10614–10621, 2016.
- [26] P. Tripathi, E. Mitsari, M. Romanini, P. Serra, J. Ll. Tamarit, M. Zuriaga, and R. Macovez, “Orientational relaxations in solid (1,1,2,2)-tetrachloroethane,” *The Journal of Chemical Physics*, vol. 144, no. 16, p. 164505, 2016.
- [27] B. Ben Hassine, P. Negrier, M. Romanini, M. Barrio, R. Macovez, A. Kallel, D. Mondieig, and J. L. Tamarit, “Structure and reorientational dynamics of 1-f-adamantane,” *Phys. Chem. Chem. Phys.*, vol. 18, pp. 10924–10930, 2016.
- [28] J. F. Gebbia, M. A. Ramos, D. Szweczyk, A. Jezowski, A. I. Krivchikov, Y. V. Horbatenko, T. Guidi, F. J. Bermejo, and J. Ll. Tamarit, “Glassy anomalies in the

- low-temperature thermal properties of a minimally disordered crystalline solid,” *Physical Review Letters*, vol. 119, no. 21, p. 215506, 2017.
- [29] M. Moratalla, J. F. Gebbia, M. A. Ramos, L. C. Pardo, S. Mukhopadhyay, S. Rudić, F. Fernandez-Alonso, F. J. Bermejo, and J. Ll. Tamarit, “Emergence of glassy features in halomethane crystals,” *Phys. Rev. B*, vol. 99, p. 024301, Jan 2019.
- [30] P. Negrier, M. Barrio, M. Romanini, J. Ll. Tamarit, D. Mondieig, A. I. Krivchikov, L. Kepinski, A. Jezowski, and D. Szewczyk, “Polymorphism of 2-adamantanone,” *Crystal Growth & Design*, vol. 14, no. 5, pp. 2626–2632, 2014.
- [31] D. Szewczyk, A. Jeowski, G. A. Vdovichenko, A. I. Krivchikov, F. J. Bermejo, J. Ll. Tamarit, L. C. Pardo, and J. W. Taylor, “Glassy dynamics versus thermodynamics: the case of 2-adamantanone,” *The Journal of Physical Chemistry B*, vol. 119, no. 26, pp. 8468–8474, 2015. PMID: 26073682.
- [32] M. Romanini, J. Ll. Tamarit, L. C. Pardo, F. J. Bermejo, R. Fernandez-Perea, and F. L. Pratt, “Implanted muon spin spectroscopy on 2-o-adamantane: a model system that mimics the liquid \rightarrow glasslike transitions,” *Journal of Physics: Condensed Matter*, vol. 29, p. 085405, jan 2017.
- [33] B. Cui, R. Milkus, and A. Zaccone, “Direct link between boson-peak modes and dielectric α -relaxation in glasses,” *Phys. Rev. E*, vol. 95, p. 022603, Feb 2017.
- [34] B. Cui, J. F. Gebbia, J. Ll. Tamarit, and A. Zaccone, “Disentangling α and β relaxation in orientationally disordered crystals with theory and experiments,” *Phys. Rev. E*, vol. 97, p. 053001, May 2018.
- [35] M. Baggioli and A. Zaccone, “Soft optical phonons induce glassy-like vibrational and thermal anomalies in ordered crystals,” *arXiv e-prints*, p. arXiv:1812.07245, Dec 2018.
- [36] S. F. Parker, F. Fernandez-Alonso, A. J. Ramirez-Cuesta, J. Tomkinson, S. Rudić, R. S. Pinna, G. Gorini, and J. F. Castañón, “Recent and future developments on TOSCA at ISIS,” *Journal of Physics: Conference Series*, vol. 554, p. 012003, nov 2014.
- [37] R. S. Pinna, S. Rudić, S. F. Parker, J. Armstrong, M. Zanetti, G. koro, S. P. Waller, D. Zacek, C. A. Smith, M. J. Capstick, D. J. McPhail, D. E. Pooley, G. D. Howells, G. Gorini, and F. Fernandez-Alonso, “The neutron guide upgrade of the toska spectrometer,” *Nuclear Instruments and Methods in Physics Research Section A: Accelerators, Spectrometers, Detectors and Associated Equipment*, vol. 896, pp. 68 – 74, 2018.
- [38] R. Zwanzig, “Nonlinear generalized langevin equations,” *Journal of Statistical Physics*, vol. 9, pp. 215–220, Nov 1973.
- [39] B. Cui and A. Zaccone, “Generalized langevin equation and fluctuation-dissipation theorem for particle-bath systems in external oscillating fields,” *Phys. Rev. E*, vol. 97, p. 060102, Jun 2018.
- [40] J. Wuttke, “Laplacefourier transform of the stretched exponential function: Analytic error bounds, double exponential transform, and open-source implementation libkww,” *Algorithms*, vol. 5, no. 4, pp. 604–628, 2012.
- [41] L. Sjogren and A. Sjolander, “Kinetic theory of self-motion in monatomic liquids,” *Journal of Physics C: Solid State Physics*, vol. 12, no. 21, p. 4369, 1979.
- [42] B. Cui, Z. Evenson, B. Fan, M.-Z. Li, W.-H. Wang, and A. Zaccone, “Possible origin of β -relaxation in amorphous metal alloys from atomic-mass differences of the constituents,” *Phys. Rev. B*, vol. 98, p. 144201, Oct 2018.